The Role of a Conserved Proline Residue in Mediating Conformational Changes Associated with Voltage Gating of Cx32 Gap Junctions

Yi Ri,* Juan A. Ballesteros,# Charles K. Abrams,* Seunghoon Oh,* Vytas K. Verselis,* Harel Weinstein,# and Thaddeus A. Bargiello*

*Department of Neuroscience, Albert Einstein College of Medicine, Bronx, New York 10461, and #Department of Physiology and Biophysics, Mount Sinai School of Medicine, New York, New York 10029 USA

ABSTRACT We have explored the role of a proline residue located at position 87 in the second transmembrane segment (TM2) of gap junctions in the mechanism of voltage-dependent gating of connexin32 (Cx32). Substitution of this proline (denoted Cx32P87) with residues G, A, or V affects channel function in a progressive manner consistent with the expectation that a proline kink (PK) motif exists in the second transmembrane segment (TM2) of this connexin. Mutations of the preceding threonine residue T86 to S, A, C, V, N, or L shift the conductance-voltage relation of wild-type Cx32, such that the mutated channels close at smaller transjunctional voltages. The observed shift in voltage dependence is consistent with a reduction in the open probability of the mutant hemichannels at a transjunctional voltage (V_j) of 0 mV. In both cases in which kinetics were examined, the time constants for reaching steady state were faster for T86N and T86A than for wild type at comparable voltages, suggesting that the T86 mutations cause the energetic destabilization of the open state relative to the other states of the channel protein. The structural underpinnings of the observed effects were explored with Monte Carlo simulations. The conformational space of TM2 helices was found to differ for the T86A, V, N, and L mutants, which produce a less bent helix (~20° bend angle) compared to the wild type, which has a ~37° bend angle. The greater bend angle of the wild-type helix reflects the propensity of the T86 residue to hydrogen bond with the backbone carbonyl of amino acid residue I82. The relative differences in propensity for hydrogen bonding of the mutants relative to the wild-type threonine residue in the constructs we studied (T86A, V, N, L, S, and C) correlate with the shift in the conductance-voltage relation observed for T86 mutations. The data are consistent with a structural model in which the open conformation of the Cx32 channel corresponds to a more bent TM2 helix, and the closed conformation corresponds to a less bent helix. We propose that the modulation of the hydrogen-bonding potential of the T86 residue alters the bend angle of the PK motif and mediates conformational changes between open and closed channel states.

INTRODUCTION

Gap junctions are intercellular aqueous channels that are formed by the interaction of two hemichannels or connexons present in apposed cells. Each hemichannel is an oligomer of six identical protein subunits, (termed *connexins*) that are hexagonally arranged around a large central pore (Unwin and Ennis, 1984; Casper et al., 1977; Makowski et al., 1977) estimated to be 6–7 Å in radius (Oh et al., 1997; Beblo and Veenstra 1997; Wang and Veenstra, 1997). Electron cryomicroscopy and image analysis of frozen-hydrated two-dimensional gap junction channel crystals resolve four α-helical transmembrane segments per protein subunit (Unger et al., 1997; Yeager, 1998). The accepted membrane topology places the N- and C-termini intracellularly.

In the vertebrate connexin gene family, a proline residue is conserved at the same position in the second transmembrane segment of all 15 members. Mutations of the proline residue have been shown to alter voltage-dependent gating of Cx26 (Suchyna et al., 1993). In Cx32, mutations of the P87 residue (P87A, L, and S) and flanking residues (T86A, S, and N; S85C and F) are associated with the X-linked form of Charcot-Marie-Tooth disease (see review by Bone et al., 1997), a common hereditary peripheral neuropathy that results from the loss of some aspect of Cx32 function (see Oh et al., 1997). A mutation of the same proline residue in Cx50 (P88S) is associated with hereditary zonular pulverulent cataract formation (Shiels et al., 1998) that is likely to result from Cx50 loss of function (White et al., 1998).

Proline residues are found in the transmembrane segments of many integral membrane proteins, such as receptors with structural similarity to rhodopsin, bacteriorhodopsin, and the photosynthetic reaction center, as well as transporters and ion channels (Woolfson et al., 1991; Sansom, 1992; Ballesteros and Weinstein, 1995). Conserved proline residues in these proteins have been proposed to undergo conformational changes that underlie functional transitions between active and inactive states (Ballesteros and Weinstein, 1995).

Proline residues are known to perturb the structure of transmembrane helices (TMHs) by introducing a kink, composed of a bend (Barlow and Thornton, 1988) and a twist (Ballesteros and Weinstein, 1992; Sankararamakrishnan and Vishveshwara, 1992) between the TMH segments preceding and following the proline residue. The conformations of proline kinks (PKs) in α-helices, as defined by the

Received for publication 11 December 1998 and in final form 18 March 1999.

Address reprint requests to Dr. T. A. Bargiello, Department of Neuroscience, Kennedy Center, Albert Einstein College of Medicine, 1410 Pelham Parkway South, Bronx, NY 100461. Tel.: 718-430-2575; Fax: 718-430-8821; E-mail: bargiell@aecom.yu.edu.

Drs. Ballesteros and Ri contributed equally to this work.

0006-3495/99/06/2887/12 $2.00

bond torsion angles of the peptide backbone, have been shown to be highly variable in solution (Pastore et al., 1989) and to have a relatively broad energy minimum (Piela et al., 1987; Barlow and Thornton 1988; Yun et al., 1991). Thus, in the absence of specific interactions, a PK motif has significant flexibility that enables it to adopt a number of different conformations with roughly equal probability (Pastore et al., 1989; Williams and Deber, 1991). The intrinsic flexibility of PK motifs and their ability to respond conformationally to specific interactions suggest that they may play a dynamic role by directly mediating the interconversion of different protein states. In this paper we present an approach to testing for the presence of a PK motif and evaluating its potential functional role in voltage-dependent gating of gap junctions formed by Cx32 by exploring structure-function relations in a series of constructs in which the proline kink has been modified by mutations.

MATERIALS AND METHODS

Computational simulations and analysis of known protein structures

The segment of TM2 of Cx32 from L76 to H97 was modeled as a Pro-kinked α-helix, following the methodology described by Ballesteros and Weinstein (1995). The novel technique of conformational memories (Guarnieri and Wilson, 1995; Guarnieri and Weinstein, 1996) was used to explore the conformational space available for the (PK) of TMH2. Conformational memories is a two-stage process, consisting of an exploratory phase and a biased sampling phase. In the exploratory phase, repeated Monte Carlo simulated annealing runs are performed (Kirkpatrick et al., 1983). Each simulation maps out a different random subsection of the conformational space, and merging these simulations can rapidly achieve a complete mapping of the conformational space. In the second stage, the ensembles of the populated conformational structures at 310 K are obtained by sampling only from the populated regions of the conformational memories; 500 representative structures of each TMH2 construct were selected for analysis.

The Monte Carlo simulations of the PK of TM2 were performed by varying the torsional angles of residues L79 to V91; this includes the more flexible PK motif (residues L83 to P87) plus an α-helical turn on each side of the PK. Accordingly, the variation in backbone dihedral angles ϕ and ψ was restrained to $\pm 50°$ from their initial values for residues within the PK (L83 to P87) and to $\pm 10°$ from their initial values for residues one turn above (A88 to V91) and below (L79 to I82) the PK. Side-chain dihedral angles were rotated freely. To reach convergence of the resulting conformations, between 200 and 400 rounds of independent random simulations were performed for each construct. In each round, repeated runs of Monte Carlo simulated annealing were performed from a starting temperature of $T_1 = 2070$ K, with a cooling schedule of $T_{n+1} = 0.9 \times T_n$, and 20,000 steps per temperature to reach 310 K. This implies that between 38 million and 152 million conformations were sampled for each wild-type and mutant construct. Analysis of the resulting conformations was performed at $T = 310$ K. The environment was modeled by a distance-dependent dielectric. The force field for the energy calculation is the Amber* force field as implemented in Macromodel (Mohamadi et al., 1990).

Analysis of known protein structures was performed using the Iditis software from Oxford Molecular, version 3.1.

Site-directed mutagenesis, RNA synthesis, and oocyte injection

Site-directed point mutations were constructed using oligonucleotide primers and the polymerase chain reaction. All chimeric constructs and point mutations were cloned into the plasmid vector pGEM7zf+ (Promega) and sequenced in their entirety. RNA was transcribed in vitro from linearized plasmid templates as described by Rubin et al. (1992). For oocyte expression of cloned connexins, ~50 nl of 1 ng/μl RNA was coinjected with 0.3 pmol/μl of an antisense phosophorothioate oligonucleotide complementary to *Xenopus* Cx38. This antisense oligonucleotide blocks all endogenous coupling between oocyte pairs attributable to Cx38 within 72 h (Barrio et al., 1991; Rubin et al., 1992).

Electrophysiological recordings

Macroscopic recordings from pairs of *Xenopus* oocytes were performed and data were analyzed as described by Rubin et al. (1992) and Verselis et al. (1994). Single-channel records were obtained from pairs of transfected Neuro-2a cells as described by Oh et al. (1997).

RESULTS

The experimental rationale underlying this study was 1) to examine the likelihood that the P87 residue located in the second transmembrane segment of Cx32 forms a proline kink (PK) motif and 2) to explore the potential role of the motif in voltage-dependent gating by exploring the structural and functional implications of site-directed mutants of the flanking amino acid residues.

Structural features of proline kinks in α-helices

To examine the likelihood that a proline kink motif is present in the second transmembrane segment of Cx32, the P87 residue was mutated to amino acid residues G, A, and V. These mutants were selected from an analysis of the structural characteristics of proline residues in α-helices. The structural distortion introduced by a proline residue in an α-helix, called a proline kink (PK), has both local and nonlocal components. Locally, the proline ring would clash with the backbone carbonyl of the amino acid at position $i - 4$ (relative to the proline residue) in a standard α-helical conformation. This structurally unfavorable interaction induces an opening in the helix backbone at the proline residue to alleviate the clash, as shown in Fig. 1. The opening of the helix backbone results in a significantly higher pitch between the proline residue and the residues located at $i - 3$ and $i - 4$ (relative to the proline residue) compared to a regular α-helical conformation. As a consequence, the helix-stabilizing backbone hydrogen bonds involving the carbonyls of these residues do not form, and the carbonyls of amino acid residues at $i - 3$ and $i - 4$ are unusually exposed (Woolfson and Williams, 1990; see Fig. 1). The most dramatic nonlocal effect of a PK on an α-helix is the induction of a bend, which for transmembrane proteins of known structure is $\pm 26°$ on average (see Fig. 1). The conformations that may be adopted by α-helices containing a proline residue have been shown to be highly variable, with a relatively wide energy minimum (Pastore et al., 1989), indicating the conformational flexibility of this structural motif.

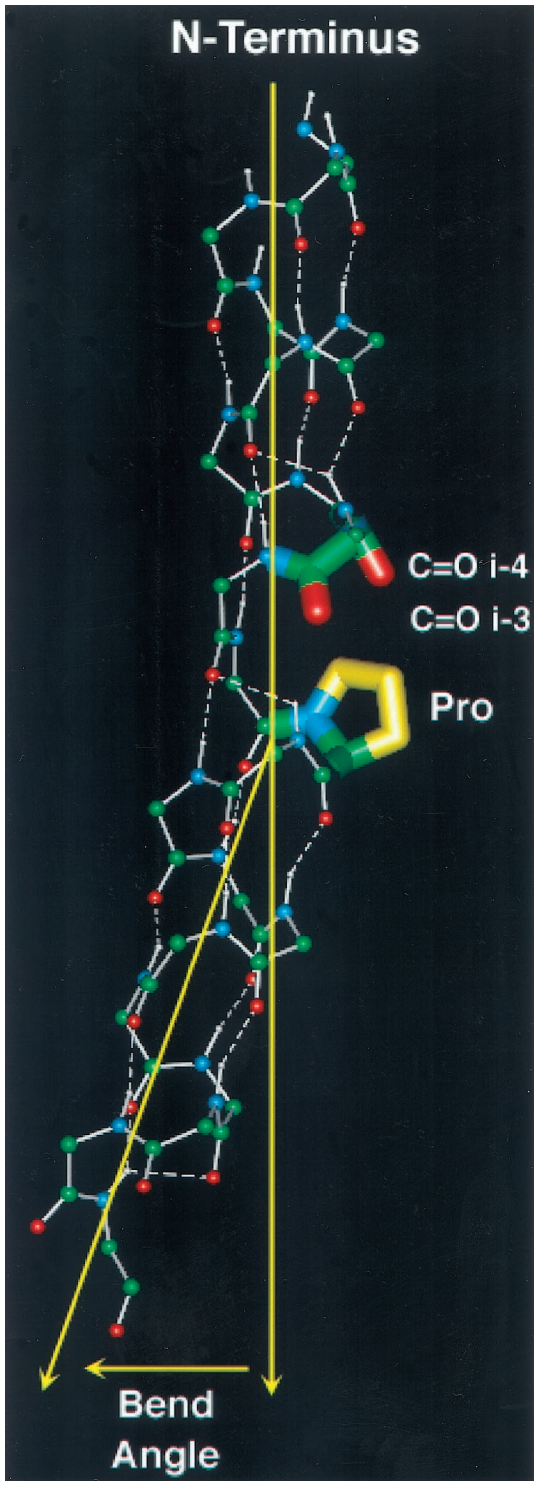

FIGURE 1 The structural features of a Pro kink motif that deviate from a standard α-helical conformation, illustrated on a molecular model of TM2 of Cx32. The Pro residue at position 87 (*yellow*) induces a bend in the α-helix, defined as the angle between the axes (*yellow*) of the helical segments preceding the Pro kink (residues 76–82) and following it (residues 88–97). The opening of the helix backbone induced by the Pro residue results in an increased solvent accessibility for the carbonyls of amino acids located at positions $i - 3$ and $i - 4$ (*liquorice bonds*) from the Pro. The hydrogen bonding pattern (*white dotted lines*) of the α-helix is broken in the Pro kink motif: the carbonyls of amino acids located at positions $i - 3$ and $i - 4$ (*liquorice bonds*) from the Pro are not H-bonded.

The structural features of a PK deviation from standard α-helical conformation can be expressed in terms of the following four quantitative parameters: 1) The degree of bending of the helix. 2) The variability of the degree of bending of the helix (also referred to as the *flexibility in bending*). 3) The solvent accessibility of the carbonyls of amino acids located at positions $i - 3$ and $i - 4$. 4) The hydrogen-bonding pattern within a helix containing a PK motif. Table 1 lists the values obtained for these parameters from our Monte Carlo (MC) simulations, found in agreement with known protein structures (see footnotes to Table 1). These results show that the set of structural parameters can differentiate between PK and standard α-helical conformations.

Computational simulations were carried out to examine the potential effects of P87G, A, and V substitutions on the structure of the TM2 helix of Cx32. We used a Monte Carlo procedure combined with simulated annealing and the application of the novel technique of conformational memories (see Materials and Methods). This procedure provides a set of 500 representative conformations of the Cx32 TM2 PK, from which any conformational preferences can be analyzed. The results of these analyses (Fig. 2) show that all three mutants are expected to adopt a standard α-helical conformation, with an average bend angle centered at zero. However, the P87V construct had a substantially decreased range in the bend angle, compared to the P87G and P87A helices. The value of the parameters described above characterizing a Pro kink motif for the P87G, A, and V substitutions on the structure of the TM2 helix of Cx32 is shown in Table 1. The variation in the structural parameters estab-

TABLE 1 Quantitative parameters characterizing the structural features of a Pro kink that deviate from a standard α-helical conformation

	Bend angle*	Flexibility in bending#	Solvent accessibility§ $C{=}O_{i-4}$, $C{=}O_{i-3}$	H-bonding pattern¶ $C{=}O_{i-4}$, $C{=}O_{i-3}$
Pro	26°	5.7	8	$C{=}O_{i-4}$ free $C{=}O_{i-3}$ 45% free
α-helix	0°	10.8	1.8	α-helix
Gly	0°	11.2	3.5	α-helix
Ala	0°	10.8	1.8	α-helix
Val	0°	8.8	0.7	α-helix

Values were calculated from an analysis of our Monte Carlo (MC) simulations, in agreement with previous analysis of known protein structures (see other table footnotes).

*Bend angle measured from the MC simulations as illustrated in Fig. 1 and defined by Barlow and Thornton (1988).

#The values are the standard deviation of the mean bend angle shown in column *, obtained from our MC simulations. The value for Ala is used as a standard α-helix.

§Solvent accessibility measured as $Å^2$ from our MC simulations, in agreement with previous analysis of known Pro kink structures (Woolfson and Williams, 1990).

¶Percentage of α-helical (i, $i + 4$) backbone H-bonding from the MC simulations. Values are in agreement with PK from known protein structures (Barlow and Thornton, 1988; Woolfson and Williams, 1990).

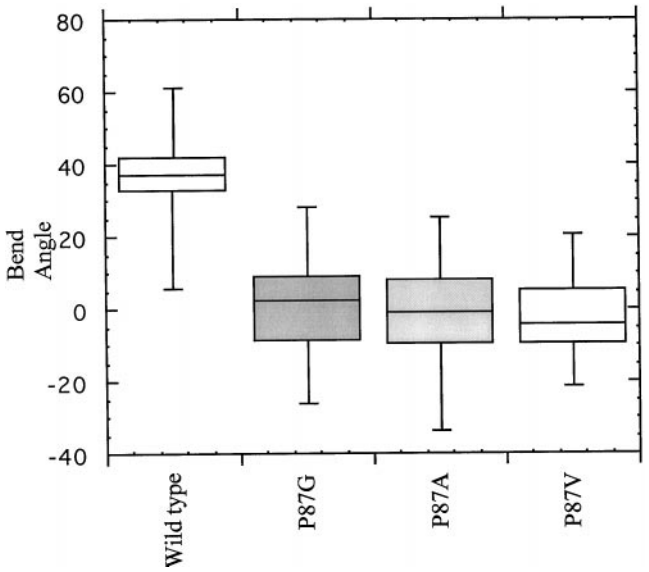

FIGURE 2 Bend angle of the Pro kink for wild type and P87 mutants. The middle line represents the median bend angle of 500 representative conformations of each TM2. Each box encloses 50% of the bend angles. The lines extending from the top and bottom of each box represent the minimum and maximum bend angles. The mean bend angles are as follows: wild-type, 37.4°; P87G, 0.5°; P87A, 0.9°; P87V, 2.5°.

lishes a rank order of departure from the standard α-helix in which Pro is at one extreme both for bending values and for solvent accessibility of the C═$O_{i-3,i-4}$ carbonyls. In this ranking, proline is followed by Gly, which allows high C═$O_{i-3,i-4}$ solvent accessibility at that position (ranking midway between a PK and a standard α-helix). The values obtained for TMHs containing alanine residue are similar to those obtained for standard α-helices. Finally, at the other extreme of the rank order is Val, which produces the lowest solvent accessibility for the carbonyl $i - 4$ and the lowest variability in bending. The structural properties characteristic of TMHs containing valine residues are due to the C^{β}-branched character of the valine residue. In α-helical environments, the conformations of valine are restricted to one rotamer population due to steric hindrances with the backbone of the preceeding turn (McGregor et al., 1987). The conformational restriction of the valine side chain imparts local rigidity to the α-helix, and in this conformation a γ-methyl group protrudes toward the preceding turn, thereby shielding the C═O_{i-4} from the solvent. Given the range of structural properties expected for TMH constructs incorporating G, A, and V at the position of the proline, these mutations were selected to probe for the presence of a PK because, as shown in Table 1, they represent middle and extreme values for these structural parameters. Thus, if a proline residue forms a PK motif in a TMH, then the substitution of these residues for proline could be expected to result in progressively greater structural changes (G $\leq$ A $<$ V), which should correlate with the degree of functional disturbance measured experimentally.

Voltage dependence of Cx32P87 mutations

Fig. 3 *A–C* illustrates that the transjunctional voltage dependence of homotypic gap junctions formed by both P87G and P87A mutations is similar to that of wild-type Cx32 homotypic junctions. The steady-state conductance of Cx32 homotypic junctions (Fig. 3 *A*) decreases to a minimum at large transjunctional voltages, resulting in a minimum conductance (defined as G_{min}) of ~0.3 times the maximum value (defined as G_o). G_{min} is not affected by the P87G substitution, but appears to be somewhat reduced by P87A to a value of ~0.2 times G_o. The subtle effects of P87G and P87A mutations on voltage dependence are more evident in the conductance-voltage relations of heterotypic pairings of the mutants with wild-type Cx32 (Fig. 3, *D* and *E*). Because of the negative gating polarity of Cx32 hemichannels (Verselis et al., 1994), the conductance-voltage relation of the mutant hemichannel corresponds to the change in conductance shown at the relatively positive limb of the conductance-voltage relation. The conductance-voltage relation

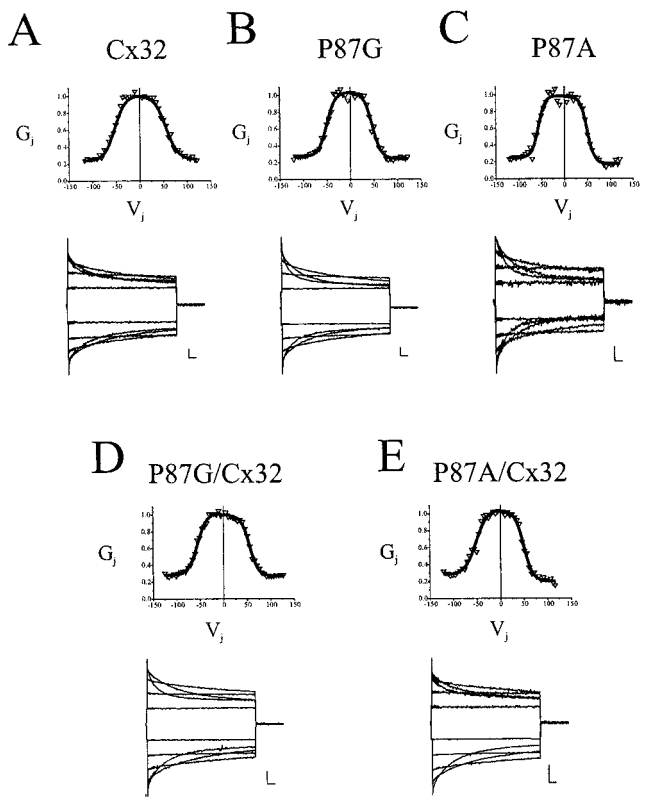

FIGURE 3 Normalized steady-state conductance-voltage relations and representative current traces of wild-type Cx32 and Cx32 P87 mutations expressed in pairs of *Xenopus* oocytes. (*A*) Cx32 homotypic junctions. (*B*) P87G homotypic junctions. (*C*) P87A homotypic junctions. (*D*) P87G/Cx32 heterotypic junctions. (*E*) P87A/Cx32 heterotypic junctions. In all cases, positive V_j is the relative positivity at the cytoplasmic entrance of the hemichannel appearing on the right side of the channel designation. Thus, in the heterotypic junctions, the *x* axis gives the V_j of the Cx32 hemichannel. Solid lines are fits of the steady-state currents to a Boltzmann relation; open triangles are the averaged normalized conductances at each transjunctional voltage from at least three separate experiments. Scale bars for current traces are 10 nA and 2 s.

of Cx32P87G/Cx32 is essentially symmetrical about $V_j = 0$ and very similar to that of homotypic Cx32 junctions. The conductance-voltage relation of the Cx32P87A/Cx32 heterotypic junction displays an asymmetry that is attributable to a small inward shift in the conductance-voltage relation of the mutant hemichannel, closing at lower transjunctional voltages, and a decrease in G_{min} (Fig. 3 *E*). These results suggest that P87A may have altered the structure of TM2 more than P87G did, but neither substitution is likely to have caused substantial conformational changes.

The latter interpretation is supported by the single-channel behavior of the P87A mutation. Three segments of a continuous single-channel recording of a homotypic P87A channel are shown in Fig. 4. The conductance of the fully open channel, 70–75 pS, does not differ substantially from the value we have reported for wild-type Cx32, ~70 pS (Oh et al., 1997). However, in agreement with the reduction in G_{min} observed macroscopically, the conductances of P87A substates appear to be somewhat reduced, ranging from 5 to 20 pS in P87A as compared to 10 to 25 pS in wild-type channels (see also Moreno et al., 1994). This result suggests that the conformations of the substates of the P87A channel have been changed. The similarity of the unitary conductance of the P87A channel to that of wild type does not preclude the possibility that the conformation of the open state may also be changed. In fact, the P87A mutation is associated with a hereditary peripheral neuropathy, X-linked Charcot-Marie-Tooth (CMTX) disease (see Bone et al., 1997). It is likely that the P87A mutation, like another Cx32 CMTX mutation, Cx32S26L, produces a subtle conformational change in the fully open channel state that reduces the permeability of large molecules without substantially changing the permeability of small ions (Oh et al., 1997).

In contrast to P87G and P87A, the P87V mutation does not express junctional currents in *Xenopus* oocytes when paired homotypically or heterotypically with either Cx32 or Cx26 ($n = 10$). The failure to observe junctional currents in either heterotypic pairing configuration may be explained by a large shift in the steady-state conductance-voltage relation of the mutant hemichannel such that the channel resides in a closed conformation at all transjunctional voltages examined (±125 mV). Alternatively, the mutant hemichannel may induce a structural change, which precludes its insertion into the membrane. In either case, it is reasonable to conclude that P87V causes a major conformational change, as predicted by the structural analyses. The near-wild-type voltage dependence of P87G and P87A mutations and the failure of P87V to express junctional currents are consistent with the interpretation that this residue forms a PK in the second transmembrane segment of Cx32.

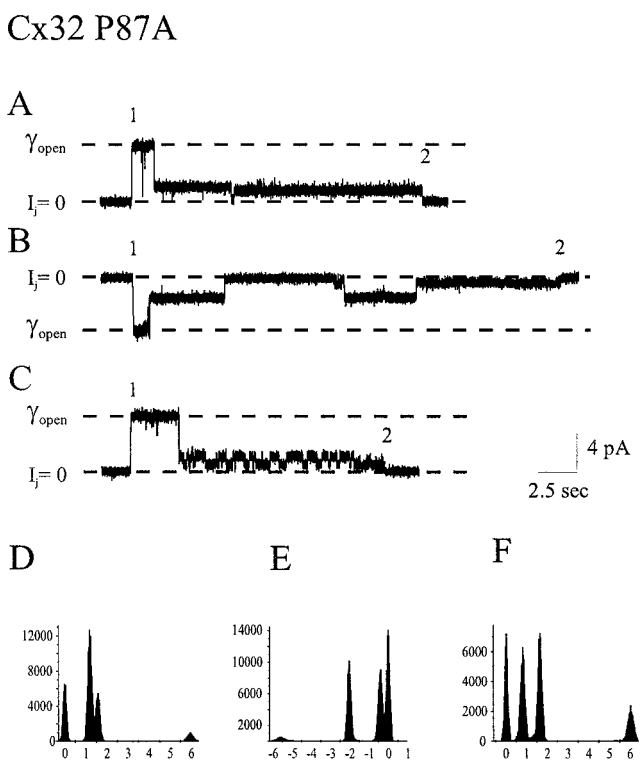

FIGURE 4 Single-channel recording of P87A mutations in transfected Neuro-2a cell pairs. (*A–C*) Segments of a continuous single-channel recording. Each member of a cell pair coupled with a single P87A homotypic channel was voltage clamped at 0 mV holding potential. In *A*, at position 1, a transjunctional voltage step of −80 mV was applied from an initial holding potential, and junctional currents were recorded from the unstepped cell, resulting in a positive current deflection. In all panels, the voltage applied to the stepped cell was returned to 0 mV at position 2. In the trace shown in *B*, a transjunctional voltage of +80 mV was applied at position 1, resulting in a negative current deflection, and in *C* a −80-mV transjunctional step was applied at position 1. (*D–F*) All point histograms of the traces shown in *A–C*, respectively. Data were acquired using Axon amplifiers and Pclamp software with a sampling frequency of 5 kHz and filtered at 1 kHz with a four-pole Bessel filter. The current traces were digitally filtered at 200 Hz for presentation. All point histograms were constructed with a bin size of 0.05 pA and fit to Gaussians, using Origin 4.0 software (Microcal Software).

Computational analysis of the structure of wild-type and mutant TM2 helices

Based on the above results, the second transmembrane segment two (TM2) of wild-type Cx32 was modeled as a proline-kinked (PK) α-helix (see Fig. 1). The range of conformations that may be adopted by the wild-type helix was explored with the Monte Carlo procedure described above, using an initial bend angle of 26°. As shown in Fig. 5, the TM2 of Cx32 behaves like a proline-kinked α-helix, adopting a range of possible PK conformations characterized by different bend angles. The average bend angle of the TM2 PK after these simulations is 37.35° (Fig. 5 *B*), a value significantly higher than the average bend angle of 26° found for PKs in known protein structures (Barlow and Thornton, 1988). Another significant feature of the simulated TM2 PK structures is the constant presence of a hydrogen bond between the side-chain OH of T86 and the backbone carbonyl of I82 (Fig. 5 *A*).

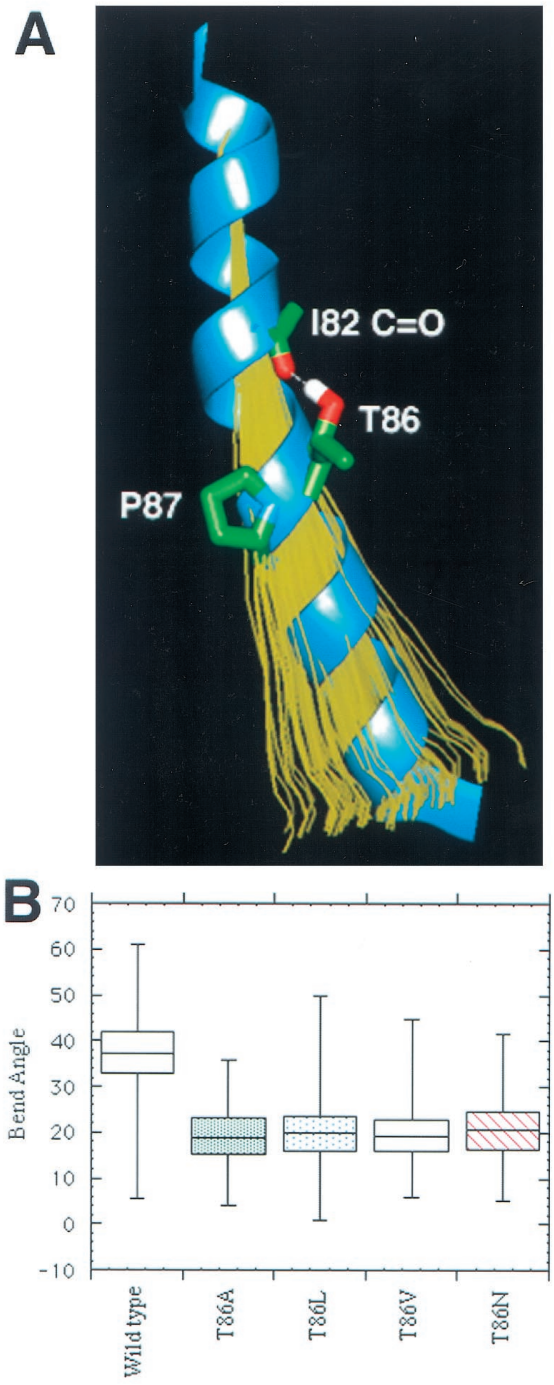

FIGURE 5 Results from the Monte Carlo simulations of TM2 of Cx32 wild type. (*A*) The backbone of TM2 (*blue*), illustrating the average bend induced by P87. The helix axes of 100 representative conformations resulting from the simulations are shown in yellow, illustrating the range of conformational freedom induced by the Pro kink. This range of Pro kink conformations is modulated by H-bonding of the hydroxyl side chain of T86 to the carbonyl of I82 (*liquorice bonds*). (*B*) Bend angle of the Pro kink for wild type and T86 mutants. The middle line represents the median bend angle of 500 representative conformations of each TM2. Each box encloses 50% of the bend angles. The lines extending from the top and bottom of each box represent the minimum and maximum bend angles. Mean bend angles are as follows: wild-type, 37.4°; T86A, 19.2°; T86L, 20.1°; T86V, 19.5°; T86N, 21.0°.

A search of known protein structures contained in the Brookhaven Protein Databank (PDB) indicated that at least 85% (204/239) of all threonine residues found in α-helices hydrogen bond to the backbone carbonyl ($C{=}O_{i-4}$) of the fourth preceding residue (Gray and Matthews, 1984). This is because the first dihedral angle of the side chain (χ_1) of threonine residues preferentially adopt a *gauche*+ rotamer ($g+ \sim -60°$) conformation. This general observation is faithfully reproduced in the Monte Carlo simulations by the hydrogen bonding of T86 to the backbone carbonyl of I82. The hydrogen bond spans the PK in TM2, which is defined as the turn preceding the proline residue, i.e., residues L83–P87 (see Fig. 5 *A*). Therefore, the T86–I82 hydrogen bond provides an additional constraint on the structure of the Cx32 TM2 PK that could be responsible for the increased bend angle observed in this particular PK. To test this hypothesis, we mutated the T86 residue to S, C, A, V, L, and N, and performed in parallel a computational exploration of the possible changes in the conformational space of TM2 incorporating these mutants.

Serine and cysteine residues are similar to threonine in that they are also capable of hydrogen bonding the backbone $C{=}O_{i-4}$ of their fourth preceding residue by adopting the $\chi_1 = g+$ rotamer conformation (Gray and Matthews, 1984). We searched the PDB to examine the preferred conformation of serine and cysteine residues in proteins with known α-helical structure. The results of this search indicated that serine residues hydrogen bond the backbone carbonyl of the preceding fourth residue by adopting the $\chi_1 = g+$ rotamer conformation in 53% (130/244) of the cases. The *trans* (i.e., $\chi_1 \sim 180°$) and $g-$ ($\chi_1 \sim 60°$) rotamers of serine were populated 29% and 18% of the time, respectively. Therefore, the mutant T86S is expected to mimic the role of the wild-type T86 in only one of three rotamer conformations that it is likely to adopt. Cysteine residues in α-helices adopt the $\chi_1 = g+$ rotamer in 61% of the cases (42/61) and adopt the *trans* configuration in 31% of the cases. The T86C mutant could also partially emulate T86 in its hydrogen-bonding potential. However, as the strength of the hydrogen bond formed by the SH group of Cys is much weaker than the strength of the hydrogen bond of the OH group of Thr and Ser residues, the T86C mutant is predicted to be much less effective than either T86 or S86 in increasing the TM2 PK bend angle. Consequently, the mean bend angles of T86S and T86C helices are expected to be less than that of wild type.

Mutations of T86 to A, V, and L remove the hydrogen bonding potential of T86. T86A should behave like a "null (loss of function) mutation," as alanine effectively removes the threonine side chain. The side chain of valine is isosteric with threonine although more hydrophobic, and leucine has a volume similar to that of valine, but the two residues are not isosteric. The substitution of asparagine (T86N) provides hydrogen bonding potential, but at a different position along the side chain than does T86 (see below). As a result, T86N would not participate in hydrogen bonding with the backbone carbonyl of I82, as would T86, T86S, and T86C.

Therefore, T86A, N, V, and L substitutions are not expected to adopt the greater bend angle of the wild-type T86 TM2, whereas T86S and C should partially emulate the wild-type helix.

The median bend angles for TM2 helices observed from the Monte Carlo simulations of the T86 mutants are shown in Fig. 5 *B*. The bend angle of all mutants (T86A, N, V, L) that cannot hydrogen bond the backbone carbonyl of residue I82 are substantially decreased from that of wild type, averaging ~20° rather than ~37° of wild type (T86). The predicted bend angle of mutant TM2 helices is close to the average angle observed for PKs in known structures (26°) (Barlow and Thornton, 1988).

In summary, the greater bend angle of wild-type TM2 PK is correlated with the ability of the threonine residue to hydrogen bond with the backbone carbonyl oxygen of amino acid I82 (Fig. 5 *A*). The decreased bend angle in the mutants (Fig. 5 *B*) is most likely a consequence of the loss of this hydrogen bond.

Voltage dependence of T86 mutants

The relative changes in the voltage dependence caused by T86 mutations are most readily observed in heterotypic pairings of the mutations with wild-type Cx32 (Fig. 6). In these plots, the V_j dependence of the mutant hemichannel can be inferred from the limb of the steady-state conductance relation at relatively positive V_j (i.e., when positive voltages are applied to the cell expressing the Cx32 hemichannel). In all cases, the steady-state conductance-voltage relations of the mutant hemichannels are shifted negatively along the voltage axis and G_{min} is reduced. The conductance-voltage relation of T86L displays the largest shift. In this case, junctional conductance is detectable only when transjunctional voltage is more negative than −60 mV. T86S displays the smallest shift in its conductance-voltage relation. The shifts in the conductance-voltage relations of the remaining T86 mutations are intermediate and follow the progression L > V > N ≥ C ≥ A > S ≥ WT. A similar progression can be inferred from shifts in the steady-state conductance-voltage relations of mutants in homotypic pairing configurations (not shown).

Unlike wild-type Cx32 homotypic junctions, the conductance-voltage relations of heterotypic junctions containing T86 mutations are not at maximum when $V_j = 0$, but the voltage at which conductance is at maximum is shifted to negative transjunctional voltages. For the most part the shift in maximum conductance and the reduction in conductance at $V_j = 0$ reflect the degree to which the conductance-voltage relation of the mutant hemichannels has been shifted along the V_j axis. We (Oh et al., 1997) have shown previously that the open probability of wild-type Cx32 single channels approaches unity in the absence of transjunctional voltages ($V_j = 0$), and consequently it is likely that almost all of the wild-type Cx32 hemichannels in homotypic and heterotypic pairings are fully open at $V_j = 0$.

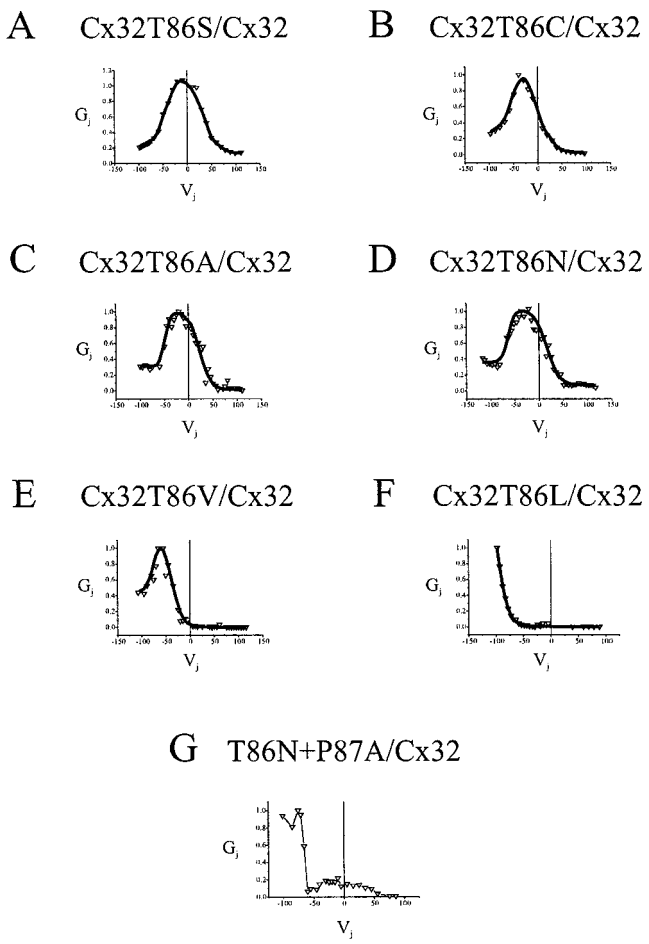

FIGURE 6 Normalized steady-state conductance-voltage relations of T86 mutations in heterotypic pairing configurations with Cx32. In all cases the value of V_j plotted is relative to the cell expressing Cx32. (*A*) Heterotypic T86S/Cx32. (*B*) Heterotypic T86C/Cx32. (*C*) Heterotypic T86A/Cx32. (*D*) Heterotypic T86N/Cx32. (*E*) Heterotypic T86V/Cx32. (*F*) Heterotypic T86L/Cx32. (*G*) Heterotypic T86N + P87A/Cx32. In *A–F*, open triangles are mean conductances obtained from at least three different oocyte pairs, and solid lines are fits of data. In *G*, the conductance-voltage relation is representative. No attempts were made to fit the data.

The simplest interpretation of the nonmaximum conductance of the wild-type/mutant heterotypic junctions at $V_j = 0$ is that the open probability of the mutant hemichannel has been reduced at this voltage. It is likely that the open probability of T86L hemichannels approaches zero at $V_j = 0$ and that other T86 mutations have intermediate open probabilities with the progression WT ≥ S > A ≥ C ≥ N > V > L. The inferred reduction in open channel probability of the mutant hemichannels at $V_j = 0$ could have resulted from either a destabilization of the open state or an increase in the stability of one or more of the "closed" states.

To further address this issue, we compared the time constants of the current relaxations of homotypic wild-type, T86A, and T86N junctions. Representative current relaxations and plots of the time constants as a function of V_j are shown in Fig. 7. Both T86A and T86N mutations display marked increases in closing kinetics relative to wild-type

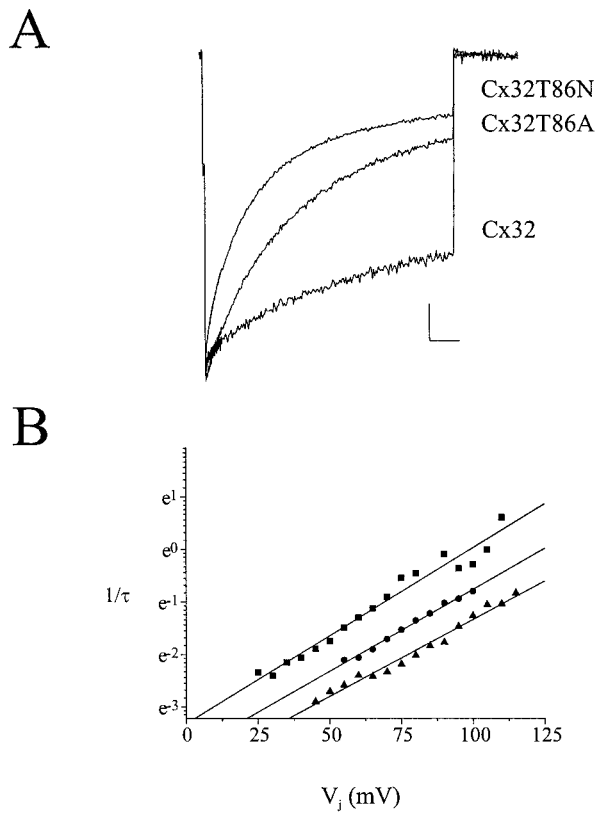

FIGURE 7 Normalized current relaxations and time constants of wild-type Cx32, T86A, and T86N. (*A*) Representative current relaxations at V_j = 60 mV. Scale bar 10 nA, 2 s. (*B*) Semilogarithmic plot of the inverse of the time constant as a function of transjunctional voltage for wild-type Cx32 (▲), T86A (●), and T86N (■).

Cx32. Although the existence of multiple subconductance states potentially complicates a simple interpretation, the observed change in time constants is consistent with an increase in the closing rate constants, which suggests that the mutations caused an increase in the free energy of the open state relative to other states of the channel. This destabilization of the open state increases the probability that the mutant channels would adopt a "closed" conformation (i.e., enter a subconductance state) at $V_j = 0$.

The interpretation of the effect of the T86N substitution as a "loss of function mutation" is complicated by the potential of asparagine to form novel hydrogen bonds. A likely hydrogen bonding partner is the backbone carbonyl of residue L83 located at position $i - 4$ from P87. Carbonyls at this position in PK motifs have been shown to be hydrogen bonding free and highly exposed (Woolfson and Williams, 1990; see Fig. 1). To investigate whether the change in voltage dependence of T86N results from the formation of a hydrogen bond to the carbonyl of L83 rather than the loss of the hydrogen bond of wild-type T86 to the carbonyl of residue I82, we constructed the double mutation Cx32T86N, P87A. As discussed above and shown in Table 1, P87A would decrease the surface accessibility of C═O_{i-4}. Therefore, the double mutation Cx32T86N, P87A would interfere with the potential hydrogen bonding of T86N to the carbonyl of L83, and the phenotype of the double mutation Cx32T86N, P87A is expected to revert to that of P87A (nearly wild type). Contrary to this expectation, the steady-state voltage dependence of the double mutation (Cx32T86N, P87A) did not revert to wild type but displayed a substantially larger shift in its conductance-voltage relation than did P87A, when paired heterotypically with Cx32 (Fig. 6 *G*). Cx32T86N, P87A did not express junctional currents when paired homotypically. This observation is consistent with the large shift in the conductance-voltage relation inferred for the mutant hemichannel. This shift would preclude the measurement of junctional currents in a homotypic pairing, as the open probability of either or both of the apposed hemichannels would approach zero at any given transjunctional voltage. Thus it appears that the shift in the steady-state conductance-voltage relation of T86N results from the loss of the hydrogen bonding potential of the wild-type T86 residue to the carbonyl of amino acid I84 rather than the formation of a novel hydrogen bond to the carbonyl of residue L83.

The near-wild-type conductance-voltage relation of the T86S mutation and greater shift in the conductance-voltage relation of T86C correlates with the hydrogen bonding potential of these substitutions. The larger shifts in the conductance-voltage relation of substitutions that cannot hydrogen bond are also consistent with the structure-related predictions. However, the relative magnitude and progression of the shifts cannot be predicted by the modeling procedure that considers the second transmembrane helix in isolation. The degree to which these mutations shift the conductance-voltage relation (A ≤ N < V < L) is probably related to other factors, such as contacts with other residues in other helices and/or the bulk and hydrophobicity of the substitution.

DISCUSSION

Structural implications of TM2 mutations

P87 mutations provide support for the existence of a proline kink motif in Cx32

The effects of amino acid substitutions at the P87 residue of Cx32, indicating a trend of functional disturbance (G ≤ A < V), are consistent with the existence of a proline kink motif in the second transmembrane segment of wild-type Cx32. The wild-type voltage dependence observed for Cx32P87G is not unexpected, as the substitution of glycine at this position is not predicted to significantly decrease the flexibility of the TMH or the surface accessibility of the carbonyls C═$O_{i-3,i-4}$. Therefore, tertiary structure interactions that may oppose the propensity for P87G to adopt a regular hydrogen-bonded structure are likely to dominate. The Cx32P87A mutant should impose stronger structural restrictions because the C^{β} moiety should decrease the surface accessibility of C═$O_{i-3,i-4}$ more than P87G and favor the adoption of a regular hydrogen-bonding pattern in

this region. The slightly greater shift in the conductance-voltage relation of the Cx32P87A hemichannel observed in the heterotypic pairings with Cx32 and the decrease in G_{min} are consistent with the structural prediction. Also as expected from the structural analyses, Cx32P87V displayed the greatest functional disturbance, as the substitution of valine should impose the greatest structural perturbation. The C^{β} moiety of valine should decrease the surface accessibility of $C{=}O_{i-3,i-4}$ even more than either glycine or alanine substitutions. In addition, valine is significantly restricted to one rotamer population due to steric hindrances caused by the C^{β}-branched character; this by itself restricts the number of conformational states that may be adopted. Consequently, Cx32P87V would have the greastest propensity to form a regular α-helix.

The expectations from the structural analysis were quantified by results from the Monte Carlo simulations performed in this study, which indicated that all three amino acid substitutions of the proline residue favor the adoption of an α-helical conformation. However, the range of energetically equivalent bend angles for Cx32P87G and Cx32P87A was shown to be greater than that of Cx32P87V. This greater conformational range of TM2 helices containing glycine and alanine subsitutions can explain the wild-type voltage dependence of Cx32P87G and Cx32P87A if one proposes that the interaction of TM2 with other domains is sufficiently strong to allow these mutant TM2s to adopt conformations that do not differ substantially from wild type. However, the substantial decrease in the range of bend angles that is predicted for P87V TM2 can be interpreted to mean that the conformational space of P87V TM2 is less than that of either glycine or alanine subsitutions. Consequently, the failure to observe junctional currents in Cx32P87V junctions may reflect the inability of interhelix interactions to overcome the propensity of the P87V TM2 to adopt an α-helix. The conformation of the open state of Cx32 thus appears to lie outside the range of energetically favorable conformations that can be adopted by P87V. It is possible that the failure of P87V to express junctional currents reflects a large shift in the conductance-voltage relation of each of the two mutant hemichannels that form the intercellular channel. Consequently, because of the serial head-to-head arrangement of hemichannels, the homotypic junction could be closed at all transjunctional voltages. This interpretation is consistent with a model in which the closed conformation of the channel would result from a transition to a less bent helix, as this would be the preferred conformation of the P87V TM2.

The difference in the behavior of proline substitutions in Cx32 from those reported by Suchyna et al. (1993) is interesting in this light. In Cx26, P87G and P87A substitutions cause large shifts in the conductance-voltage relations and appear to reverse the gating polarity of Cx26 hemichannels. These effects are consistent with the occurrence of substantial changes in the structure of Cx26 hemichannels or in the function of the P87 residue. Recent studies (Ri, Verselis, and Bargiello, unpublished) have mapped the difference in the behavior of P87G and P87A substitutions in Cx26 and Cx32 to the second transmembrane domain. The substitution of the Cx26TM2 containing P87G substitution into Cx32 (Cx32*Cx26TM2 + P87G) causes a reversal of Cx32 gating polarity analogous to the reversal of Cx26 gating polarity by Cx26P87G. Remarkably, there are only two amino acid differences in the second transmembrane segment of the two connexins (Cx32S78-Cx26A78 and Cx32L83-Cx26M83). Although it is possible that the difference in the sequence of the two connexins changes some aspect of intrahelical interactions of the two connexins and alters the conformation of the PK motif, it seems more likely that the difference in the behavior of P87 substitutions results from a difference in the interhelical interactions of TM2 in the two connexins. We propose that favorable interhelical interactions in Cx32 are sufficient to overcome the propensity of P87G or P87A mutants to adopt a less bent conformation in Cx32, whereas the interhelical interactions in Cx26 are not sufficient.

The agreement between the expected rank order of structural perturbation of the proline mutants, $G \leq A < V$, that emerged from the comparative analysis of PK motifs and α-helices found in many different known protein structures (Table 1) and the experimentally derived phenotypes supports our selection of these three mutants to probe the presence of a PK motif. Indeed, the 7-Å-resolution structure of connexin 43 solved recently by Yeager and co-workers shows four α-helical transmembrane segments, with one pore-lining helix being substantially bent (Unger et al., 1999). It is likely that this bent helix is TM2, as only the second transmembrane of segment of connexins contains a proline residue. This structural confirmation of a prediction based on the general principles inferred from a broad analysis of PK motifs suggests that the sequence of mutations of P to G, A, and V may serve as a general approach to test for the presence of a PK motif in helical transmembrane segments.

The loss of the hydrogen bonding potential of wild-type T86 appears to underlie the shift in conductance-voltage relation of T86 mutations

The Monte Carlo simulation and experimental data we present indicate that hydrogen bonding potential of the wild-type T86 residue is a major determinant in the structure-function relation of the PK motif. The large bend angle of the wild TM2 helix predicted by the Monte Carlo simulation most likely results from the formation of a hydrogen bond between the OH group of threonine residue and the backbone carbonyl of residue I82. The hydrogen bonding of the threonine side chain to the backbone carbonyl of the fourth preceding residue is the conformation adopted by 85% of threonine residues in α-helices of known protein structures. It is interesting to note that a similar TP motif exists in TM3 of bacteriorhodopsin, where the threonine side chain has the same hydrogen bonding interaction with the backbone carbonyl at residue $i - 4$, and that TM3 is also

significantly more bent than other PK TM segments (Grigorieff et al., 1996; Pebay-Peyroula et al., 1997), which are not preceded by a threonine residue. The alanine, asparagine, valine, or leucine substitions of the wild-type T86 residue cannot form this hydrogen bond in TM2 of Cx32, so that helices containing these subsitutions are predicted to adopt a less bent configuration. The observed shift in voltage dependence of these mutations, which most likely reduces their open channel probability at $V_j = 0$, is consistent with the inferred mechanistic role of the (i, $i - 4$) hydrogen bond.

In contrast, the T86S subsitution, like wild type, can hydrogen bond the backbone carbonyl of residue I82, but it does so in only one of three possbile rotamer conformations. In the two other rotamer conformations, the serine residue may have different hydrogen bonding interactions, and thus the T86S subsitution should only partially emulate the wild-type T86 TM2. The small shift in the steady-state conductance-voltage relation of this mutation is thus consistent with the structural predictions. Also consistent is the greater shift observed in the conductance-voltage relation of T86C compared to T86S, because the hydrogen formed between the SH group of cysteine and the backbone carbonyl of residue I82 is expected to be weaker than that of a serine in position 82.

The mechanism(s) responsible for the progressively greater shift in the conductance-voltage relation of amino acids that do not hydrogen bond the backbone carbonyl of I82 ($L > V > N \geq A$) cannot be addressed by the modeling precedure employed here, because it considers the TM2 helix to be in isolation. T86A should behave like a loss-of-function mutation, and the effect of T86V should largely reflect the difference in the hydrogen-bonding potential of threonine and valine, as the two amino acids are essentially isosteric. However, the greater severity of the T86L and T86V subsitutions compared to those of T86A and T86N subsitutions are likely to be caused by other factors, in addition to the loss of the hydrogen-bonding potential of these residues. These factors might include changes in interhelical contacts related to the differences in bulk and relative hydrophobicities of these two subsitutions. Based on the recent structural determinations of Cx43 (Unger et al., 1999) and our considerations pesented above, it is likely that amino acid residues in the vicinity of P87 reside in an aqueous environment. Therefore, the larger shift in the conductance-voltage relations of T86L and T86V are probably related to the greater hydrophobicities of these substitutions.

Taken together, our results suggest that the loss of the hydrogen-bonding potential is the primary effect of T86 mutations and that other factors, such bulk and hydrophobicity, are secondary effects that further constrain the conformation of the TM2 helix.

Proposed structural changes accompanying V_j-dependent gating

The observed shift in the conductance-voltage relation of T86 mutations is consistent with a decrease in open channel probability of the mutations at $V_j = 0$. The changes in time constants are consistent with an increase in the rate constant of closure in channels formed by T86A and T86N compared to wild-type Cx32. Given that the open probability of the wild-type channel is close to 1.0 in the absence of a transjunctional potential, the apparent increase in the closing rate constant strongly suggests that the T86A and T86N mutations cause the destabilization of the open state, thereby increasing the probability that the mutant channels make a transition from the open to the closed conformation at a given transjunctional voltage. This consideration and the correlation between the direction of the observed shift in the voltage dependence and the predicted decrease in bend angle for all T86 mutations support the hypothesis that a more bent conformation of TM2 corresponds to the open channel state and that a less bent conformation corresponds to the closed channel state. This hypothesis is illustrated in Fig. 8, where the resulting average PK conformations for wild-type and mutant T86 TM2 structures are shown for two opposing subunits. We propose that in the open state, TM2 helices adopt a conformation with a 37° bend angle (*blue helices*), whereas in the "closed" (residual conductance states) the bend angle of TM2 is reduced to 20° (*red helices*). In this illustration, we depict the closed state of the

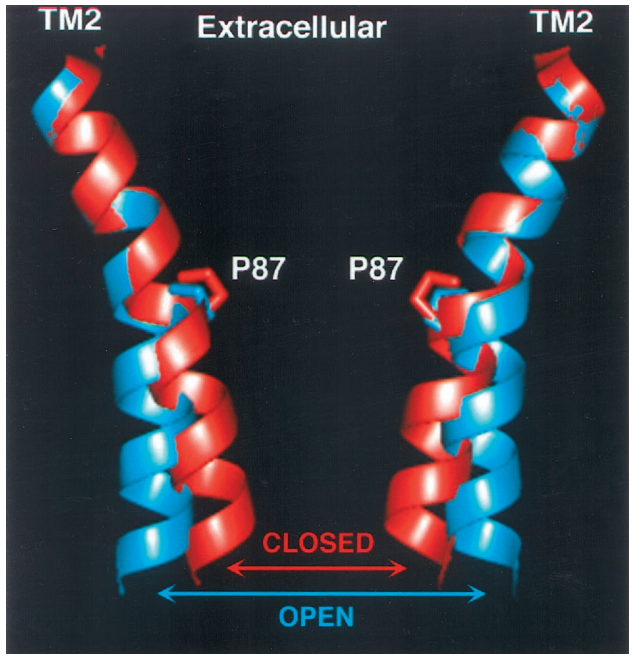

FIGURE 8 Proposed role of the Pro kink motif in TM2 of Cx32 as a flexible hinge participating in the conformational changes between open and closed states of the channel. The highly bent PK conformation of TM2 of wild-type Cx32 induced by T86 represents the open confomation of the channel (*blue*), illustrated by two TM2 segments from opposing subunits. The less bent PK conformation found for the TM2 T86 mutants of Cx32 represents the closed conformation of the channel (*red*), illustrated by two TM2 segments from opposing subunits. The extent of this conformational change is sufficient to explain channel closure, although other TM segments besides TM2 may be lining the cytoplasmic side of the channel pore (see text).

channel as arising from the movement of the C-terminal half of TM2 in a direction that would decrease the radius of the channel pore near the cytoplasmic entry. This model of V_j gating is suggested by the observed rectification of Cx32 substates, which can be interpreted to reflect an increase in the electrostatic effect of fixed charges that are located in the amino terminus (Oh et al., manuscript submitted for publication).

An estimate of the structural effect that a decrease of 17° in the PK bend angle would have on the pore radius of the hemichannel channel can be obtained from the following considerations. If the TM2 helix of Cx32 extends from R75 to H97 (22 residues), the cytoplasmic directed helical fragment P87–H97 would be 10×1.5 Å $= 15$ Å in length (as in an α-helix the pitch per residue is 1.5 Å). Consequently, the observed decrease in 17° in the bend angle of the PK in TM2 could displace the C-terminus of TM2 by 4.4 Å (i.e., 15 Å $\times$ sin 17°) toward the center of the pore to produce a decrease in the radius of the open channel from 7 Å (Oh et al., 1997) to 2.6 Å (assuming that all six connexin subunits are translocated). Assuming that the length of a hemichannel is 60 Å, and that only one of two hemichannels in series closes in response to V_j, then the substate conductance is predicted to be reduced to ~26% of that of the open state (70 pS), i.e., ~18 pS (see Hille, 1992, p. 296). This value is close to the conductance of Cx32 substates that are observed (10–25 pS; Oh et al., 1997). Thus the conformational change induced by the 17° decrease in bend angle is sufficient to explain the change in conductance resulting from the "closure" of a V_j gate.

We emphasize that the model shown in Fig. 8 is not meant to imply that the cytoplasmic half of TM2 (i.e., residues spanning P87–H97) contribute either to the channel lining or to the formation of the V_j gate. Indeed, the portion of the gap junction channel pore closer to the cytoplasm surface is formed by part of a second TM helix (Unger et al., 1999). It is likely that this helix is TM1, as Zhou et al. (1997) have demonsrated that some cysteine-substituted residues in this helix are accessible to the hydrophilic cysteine modifiying reagent MBB. We have also postulated that residue S26 in TM1 lines or is in close proximity to the channel pore (Oh et al., 1997). Thus it is feasible that the hypothesized movement of the cytoplasmic portion of TM2 displaces TM1 or the amino terminus into the channel pore, and we propose that these domains may form the "V_j gate."

Functional roles of the proline kink perturbation of the α-helix

Suchyna et al. (1993) reported that mutations of P87 altered the expression of V_j-dependent gating but not pH gating of Cx26. On this basis, they concluded that residue P87 functions as a "transduction" element in voltage-dependent gating of Cx26. Although Suchyna et al. (1993) did not explicitly define their use of the term "transduction," it is likely that they were referring to the mechanism by which the mechanical movement of one protein domain could be propagated to another, rather than the means by which electrical energy is converted into mechanical energy (i.e., the movement of the voltage sensor). Furthermore, they suggested that changes in conformation of the open and closed states resulted from *cis-trans* isomerizations of the proline residue. However, *cis*-proline isomers have not been observed in α-helices, most likely because this conformation would produce steric clashes with the backbone. Furthermore, this mechanism is unlikely, as the energy required for *cis-trans* isomerization, ~13. 5 kcal/mol (Suchyna et al., 1993), is substantially greater than the energy required to close Cx26 hemichannels. The work performed in closing 50% of a mole of Cx26 channels is ~4.4 kcal, if we assume that Cx26 has a gating valence of four charges and a $V_{1/2}$ (the voltage at which 50% of channels are closed) of ~95 mV (Verselis et al., 1994). In the case of Cx32, the work is less, ~1.5 kcal, assuming a calculated gating charge of 2 and a $V_{1/2}$ of 60 mV (Verselis et al., 1994). Notably, these values are within the range of energies required to break the proposed T86 hydrogen bond.

The intrinsic flexibility and the structural characteristics of a PK motif, which allow it to respond conformationally to specific interactions, make possible a mechanism in which the motif functions in the propagation of conformational changes from one protein domain to another. Similar mechanisms have been proposed for G-protein-coupled receptors (Luo et al., 1993; Ballesteros and Weinstein, 1995; Gether et al., 1997). The results of the Monte Carlo simulations performed in this study illustrate how substitutions of the amino acid preceding the proline residue can restrict the number of energetically favorable conformations available to a kinked α-helix and alter the preferred bend angle of the PK. We propose that H-bonding of T86 to the backbone carbonyl of I82 results in a more bent TM2 PK, which functionally corresponds to the open state of the channel. Removal of this H-bond by the T86 mutants favors a less bent TM2 PK, which functionally corresponds to the closed state of the channel.

We have previously demonstrated that charged amino acid residues located in the N-terminus and at the border of the first transmembrane segment and first extracellular loop form part of a charge complex that is likely to be an integral part of the Cx26 and Cx32 voltage sensors (Verselis et al., 1994), and that charges in the N-terminus are likely to move toward the cytoplasmic surface on channel closure. We propose that the application of a transjunctional voltage may initiate a set of molecular changes that include breaking the proposed hydrogen bond between the side chain of the T86 residue and the backbone carbonyl of residue I82. The loss of this hydrogen bond would favor a reduction in the bend angle of the PK motif, which could mediate the conformational transition from the open state to the residual conductance states of the channel.

REFERENCES

Ballesteros, J. A., and H. Weinstein. 1992. Analysis and refinement of criteria for predicting the structure and relative orientations of transmembranal helical domains. *Biophys. J.* 62:107–109.

Ballesteros, J. A., and H. Weinstein. 1995. Integrated methods for modeling G-protein coupled receptors. *Methods Neurosci.* 25:366–428.

Barlow, D. J., and J. M. Thornton. 1988. Helix geometry in proteins. *J. Mol. Biol.* 201:601–619.

Barrio, L. C., T. Suchyna, T. Bargiello, LX. Xu, R. S. Roginski, M. V. Bennett, and B. J. Nicholson. 1991. Gap junctions formed by connexins 26 and 32 alone and in combination are differently affected by applied voltage. *Proc. Natl. Acad. Sci. USA.* 88:8410–8414.

Beblo, D. A., and R. D. Veenstra. 1997. Monovalent cation permeation through the connexin40 gap junction channel. Cs, Rb, K, Na, Li, TEA, TMA, TBA, and effects of anions BR, Cl, F, acetate, aspartate, glutamate and NO3. *J. Gen. Physiol*. 109:509–522.

Bone, L. J., S. M. Deschenes, R. J. Balice-Gordon, K. H. Fishbeck, and S. S. Scherer. 1997. Connexin 32 and X-linked Charcot-Marie-Tooth disease. *Neurobiol. Dis.* 4:221–230.

Casper, D. L., D. A. Goodenough, L. Makowski, and W. C. Phillips. 1977. Gap junction strucutres. I. Correlated electron microscopy and x-ray diffraction. *J. Cell Biol*. 74:605–628.

Gether, U., S. Lin, P. Ghanouni, J. A. Ballesteros, H. Weinstein, and B. K. Kobilka. 1997. Agonists induce conformational changes in transmembrane domains III and VI of the b2 adrenergic receptor. *EMBO J.* 16(22):6737–6747.

Gray, T. M., and B. W. Matthews. 1984. Intrahelical hydrogen bonding of serine, threonine and cysteine residues within alpha-helices and its relevance to membrane-bound proteins. *J. Mol. Biol.* 175(1):75–81.

Grigorieff, N., T. A. Ceska, K. H. Downing, J. M. Baldwin, and R. Henderson. 1996. Electron-crystallographic refinement of the structure of bacteriorhodopsin. *J. Mol. Biol.* 259(3):393–421.

Guarnieri, F., and H. Weinstein. 1996. Conformational memories and the exploration of biologically relevant peptide conformations: an illustration for the gonadotropin-releasing hormone. *J. Am. Chem. Soc.* 118: 5580–5589.

Guarnieri, F., and S. R. Wilson. 1995. Conformational memories and a simulated annealing program that learns: application to LTB4. *J. Comput. Chem.* 16(5):648–653.

Hille, B. 1992. Ionic Channels of Excitable Membranes. Sinauer Associates, Sunderland, MA.

Kirkpatrick, S., C. D. Gelatt, and M. P. Vecchi. 1983. Optimization by simulated annealing. *Science.* 220:671–680.

Luo, X., D. Zhang, and H. Weinstein. 1993. Ligand-induced domain motion in the activation mechanism of a G-protein-coupled receptor. *Protein Eng.* 7:1441–1448.

Makowski, L., D. L. Casper, D. A. Goodenough, and W. C. Phillips. 1977. Gap junction structures. II. Analysis of the x-ray diffraction data. *J. Cell Biol.* 74:629–645.

McGregor, M. J., S. A. Islam, and M. J. Sternberg. 1987. Analysis of the relationship between side-chain conformation and secondary structure in globular proteins. *J. Mol. Biol.* 198(2):295–310.

Mohamadi, F., N. G. J. Richards, W. C. Guida, R. Liskamp, M. Lipton, C. Caulfield, G. Chang, T. Hendrickson, and W. C. Still. 1990. An integrated software system for modeling organic and bioorganic molecules using molecular mechanisms. *J. Comput. Chem.* 11:440–467.

Moreno, A. P., M. B. Rook, G. I. Fishman, and D. C. Spray. 1994. Gap junction channels: distinct voltage-sensitive and -insensitive conductance states. *Biophys. J.* 67:113–119.

Oh, S., Y. Ri, M. V. L. Bennett, E. B. Trexler, V. K. Verselis, and T. A. Bargiello. 1997. Changes in permeability caused by connexin 32 mutations underlie X-linked Charcot-Marie-Tooth disease. *Neuron.* 19: 927–938.

Pastore, A., T. S. Harvey, C. E. Dempsey, and I. D. Campbell. 1989. The dynamic properties of melittin in solution. Investigations by NMR and molecular dynamics. *Eur. Biophys. J.* 16(6):363–367.

Pebay-Peyroula, E., G. Rummel, J. P. Rosenbusch, and E. M. Landau. 1997. X-ray structure of bacteriorhodopsin at 2.5 angstroms from microcrystals grown in lipidic cubic phases. *Science*. 277(5332): 1676–1681.

Piela, L., G. Nemethy, and H. A. Scheraga. 1987. Proline-induced constraints in alpha-helices. *Biopolymers.* 26:1587–1600.

Rubin, J. B., V. K. Verselis, M. V. L. Bennett, and T. A. Bargiello. 1992. Molecular analysis of voltage dependence of heterotypic gap junctions formed by connexins 26 and 32. *Biophys. J.* 62:183–195.

Sankararamakrishnan, R., and S. Vishveshwara. 1992. Geometry of proline-containing alpha-helices in proteins. *Int. J. Pept. Protein Res.* 39: 356–363.

Sansom, M. S. 1992. Proline residues in transmembrane helices of channel and transport proteins: a molecular modelling study. *Protein Eng.* 5:53–60.

Shiels, A., D. Mackay, A. Ionides, A. Moore, and S. Bhattacharya. 1998. A missense mutation in the human connexin50 gene underlies autosomal dominant "zonular pulverulent" cataract, on chromosome 1q. *Am. J. Hum. Genet.* 62:526–532.

Suchyna, T. M., L. X. Xu, F. Gao, C. R. Fourtner, and B. J. Nicholson. 1993. Identification of a proline residue as a transduction element involved in voltage gating of gap junctions. *Nature.* 365:847–849.

Unger, V. M., N. M. Kumar, N. B. Gilula, and M. Yeager. 1997. Projection structure of a gap junction membrane channel at 7 Å resolution. *Nature Struct. Biol.* 4:39–43.

Unger, V. M., N. M. Kumar, N. B. Gilula, and M. Yeager. 1999. Three dimensional structure of a recombinant gap junction membrane channel. *Science.* 283:1176–1180.

Unwin, P. N., and P. D. Ennis. 1984. Two configurations of a channel-forming membrane protein. *Nature.* 307:609–613.

Verselis, V. K., C. S. Ginter, and T. A. Bargiello. 1994. Opposite voltage gating polarities of two closely related connexins. *Nature.* 368:348–351.

Wang, H. Z., and Veenstra. 1997. Monovalent ion selectivity sequences of the rat connexin43 gap junction channel. *J. Gen. Physiol*. 109:491–507.

White, T. W., D. A. Goodenough, and D. L. Paul. 1998. Targeted ablation of connexin50 in mice results in microphthalmia and zonular pulverulent cataracts. *J. Cell Biol.* 143:815–825.

Williams, K. A., and C. M. Deber. 1991. Proline residues in transmembrane helices: structural or dynamic role? *Biochemistry*. 30(37): 8919–8923.

Woolfson, D. N., S. R. J. Mortishire, and D. H. Williams. 1991. Conserved positioning of proline residues in membrane-spanning helices of ion-channel proteins. *Biochem. Biophys. Res. Commun.* 175(3):733–737.

Woolfson, D. N., and D. H. Williams. 1990. The influence of proline residues on alpha-helical structure. *FEBS Lett.* 277:185–188.

Yeager, M. 1998. Structure of cardiac gap junction intercellular channels. *J. Struct. Biol.* 121:231–245.

Yun, R. H., A. Anderson, and J. Hermans. 1991. Proline in alpha-helix: stability and conformation studied by dynamics simulation. *Proteins.* 10(3):219–228.

Zhou, X. W., A. Pfahnl, R. Werner, A. Hudder, A. Llanes, A. Leubke, and G. Dahl. 1997. Identification of a pore lining segment in gap junction hemichannels. *Biophys. J.* 72:1946–1953.